STATISTICS, OPTIMIZATION AND INFORMATION COMPUTING
Stat., Optim. Inf. Comput., Vol. **x**, Month 2025, pp 0–13.
Published online in International Academic Press (www.IAPress.org)

Optimal placement and sizing of photovoltaic generators and static reactive power compensators in distribution systems for minimizing the annual energy purchase cost using the fractional optimization algorithm

Juan Sebastián Alonso Medina, Oscar Danilo Montoya*, and Juan Diego Pulgarín Rivera

Facultad de Ingeniería, Universidad Distrital Francisco José de Caldas, Bogotá D.C. 110121, Colombia

Abstract This paper presents an innovative algorithm, termed the Fractional Optimization Algorithm (FOA), which utilizes the properties of fractional functions to enhance the integration of photovoltaic (PV) systems and distribution static compensators (D-STATCOMs) into distribution systems (DSs). The FOA employs a discrete-continuous encoding approach to determine the optimal placement and sizing of PV and D-STATCOM devices. A master-slave optimization framework is adopted, where the FOA operates in the master stage, and the successive approximations method is used for power flow analysis in the slave stage. The algorithm's efficacy is tested on 33- and 69-bus grids, demonstrating significant cost reductions over traditional optimization approaches such as the Vortex Search Algorithm (VSA) and the Sine-Cosine Algorithm (SCA). Furthermore, the FOA achieves superior computational efficiency, underscoring its promise as a robust optimization strategy.

Keywords Fractional Optimization Algorithm; Photovoltaic System; Distribution Static Compensator; Power Flow Analysis; Distribution systems.

AMS 2010 subject classifications 62J07

DOI:10.19139/soic-2310-5070-3170

1. Introduction

1.1. General context

Climate change, mainly driven by greenhouse gas emissions and along with the global increase in electricity demand, have fostered the emergence and development of distributed generation (DG) systems, based on both conventional energy sources and renewable energy resources (RES) [1], within DSs. One of the key differences between DG and conventional generation lies in the location of generation units. DG places small-scale generators close to the consumption points [2], whereas conventional generation relies on large power plants located far from end users. However, it is essential to optimize both the placement and sizing of DG units, as this enhances the technical and economic performance of the system [3].

In this context, RES have become a prominent alternative for developing environmentally friendly power systems, contributing to sustainability, reducing greenhouse gas emissions and enabling the energy transition [4], all while maintaining technical and economic efficiency. Among the available technologies, solar energy stands out due to its abundant availability and decreasing implementation costs [5]. Furthermore, to enhance the advantages of PV systems, static reactive power compensators, commonly known as D-STATCOMs, are often integrated. These

*Correspondence to: O. D. Montoya (Email: odmontoyag@udistrital.edu.co). Facultad de Ingeniería, Universidad Distrital Francisco José de Caldas, Bogotá D.C. 110121, Colombia.

ISSN 2310-5070 (online) ISSN 2311-004X (print)

devices provide a dynamic response to reactive power variations, improve voltage profiles, and reduce power losses, ultimately leading to lower electricity generation costs [6].

1.2. Motivation

The integration of PV systems and D-STATCOMs into DSs offers multiple economic, technical, and environmental benefits, which has attracted significant interest from both academia and industry [7]. For example, their coordinated deployment can lead to substantial reductions in annual investment and operational costs [8] as well as improvements in voltage profiles and power losses [9] which inevitably lead into environmental benefits. As a result, it is crucial to promote research initiatives focused on the efficient implementation of DG, aiming to maximize its benefits while minimizing negative impacts for all stakeholders involved in the generation, transmission, commercialization, and consumption of electrical energy.

Given these considerations, the integration of DG must be conducted in an optimal manner to avoid unintended adverse effects. For this reason, over the past three decades, the optimal siting of DG units has become a prominent topic in the scientific community [10]. In fact, various methods have been developed to address this issue with metaheuristic algorithms standing out for their ability to provide high quality solutions (near-optimal) to complex optimization problems [11]. Therefore, this research adopts a fractional optimization algorithm, which is classified as a metaheuristic technique, to determine the optimal placement and sizing of PV systems and D-STATCOMs, with the objective of reducing electricity purchases at the medium voltage substation.

1.3. Literature review

Several studies in the specialized literature have addressed the implementation of DG in power systems. For example, [12] presents an overview of the different DG types, their impacts, challenges and potential solutions for integration into DSs. This work focuses on two key challenges encountered in DG deployment: protection schemes and voltage control mechanisms. Similarly, [13] highlights the importance of DG planning from multiple perspectives, including the reduction of active and reactive power losses, enhancement of system reliability, improvement of voltage profiles, and the environmental benefits associated with renewable energy integration. Their study also outlines the current state of DG planning considering these factors.

In addition to case-specific studies, several review papers have analyzed the role of optimization algorithms in DG integration. [14] reviews various metaheuristic optimization techniques applied to the Optimal Reactive Power Dispatch problem in systems that incorporate renewable-based DG units. [15] presents a comprehensive analysis comparing renewable energy integration with conventional sources, while also surveying existing approaches for the optimal siting and sizing of DG units within electric power systems. [2] provides another review that categorizes the main objectives, constraints and optimization strategies considered in the optimal allocation of DG units, ultimately concluding that hybrid algorithms represent the most suitable option for solving this problem.

In terms of practical implementation of distributed energy resources (DERs) within DG frameworks, various metaheuristic techniques have been explored. For example, [16] applies the Fractional Order Kepler Optimization Algorithm to improve power efficiency and system performance, comparing its results with other optimization methods in 33- and 69-bus systems. [17] proposes the multi-objective Harris Hawks Optimization algorithm to minimize power losses and enhance voltage profiles in 69- and 118-bus networks. In the same way, [18] employs the Walrus optimization algorithm, which it is also metaheuristic algorithm, within a multi-objective framework to simultaneously reduce power losses, improve voltage profiles and ensure voltage stability, subject to operational constraints.

Furthermore, the optimal deployment of PV generators and D-STATCOMs has been examined as a means to reduce both operational and investment costs in DSs. For instance, [19] proposes a multiverse optimization algorithm combined with a matrix-based power flow solver to minimize annual investment and operational costs in 33- and 69-bus test feeders. Their findings indicate that proper sizing and placement of PVs and D-STATCOMs not only reduce total system costs but also lead to lower computational times when implemented in a programming environment.

1.4. Contributions and scope

Taking into account the literature review that has been given in this article, this research develops the implementation of a novel optimization algorithm for the location and sizing of PVs and D-STATCOMs in DS. For this, a mathematical model that allows adopting a master-slave approach is applied. At first, in the master stage, the FOA is used as the main and only solution method employing a discrete-continuous coding strategy. The discrete strategy results in the location of PVs and D-STATCOMs, while the continuous one results in their sizing. In the slave stage, the successive approximations method is used to find the feasibility of possible solutions, obeying the regulated electrical values and accurately determine the power injection into the system. The numerical results will make it possible to compare the superiority of the FOA with other algorithms such as the SCA and the VSA reported in [20].

The scope of this article covers aspects such as the development of a mathematical model that takes into account the operational constraints of the electrical system by implementing real characteristics of the DS, obtained from the corresponding utility. Actual values of the daily demand for real and reactive power at the substation terminals are also available. Furthermore, approximate solar generation profiles were developed in the region where the medium-voltage feeder is located. For a reasonable comparison, parameters identical to those presented in [20] are used.

1.5. Document structure

The structure of this article is described as follows. In section 2 the optimization model developed is introduced for optimally placement and sizing of PVs and D-STATCOMs in DS. This model employs a mixed-integer nonlinear programming (MINLP) approach which minimizes the annual energy purchase cost over a 20-year planning horizon. Section 3 explains the proposed solution methodology, which integrates the FOA with multi-period optimal power flow analysis within a master-slave framework to efficiently solve the studied problem. Section 4 provides a detailed description of the test cases, focusing on the analyzed 33- and 69-bus systems, including a parameterization of the objective functions, the network topology, and the operational constraints. In Section 5 the computational results obtained are presented, as well as a validation of the proposed methodology and comparative analyses against literature-reported results. Finally, Section 6 summarizes the key findings and highlights potential avenues for future research.

2. General MINLP formulation

In this section, we present a comprehensive mathematical model for the optimal placement and sizing of PV systems and D-STATCOMs in electrical DSs. This formulation integrates the objective function, constraints, and auxiliary equations into a unified MINLP framework, facilitating a holistic approach to the optimization challenge. The model expertly balances the need for precision in determining system components with the computational efficiency required for practical application in diverse grid scenarios.

2.1. Objective Function

The objective of the optimization model is to minimize the total energy purchasing costs, which also include investment, and maintenance expenses. This objective function is defined as follows [20]:

$$\min z_{\text{cost}} = z_1 + z_2, \tag{1}$$

where:

$$z_1 = C_{kWh} T f_a f_c \sum_{h\in\mathcal{H}} \sum_{i\in\mathcal{N}} p_{i,h}^{cg} \Delta h, \tag{2}$$

$$z_2 = C_{pv} f_a \sum_{i\in\mathcal{N}} p_i^{pv} + T \sum_{h\in\mathcal{H}} \sum_{i\in\mathcal{N}} C_{O\&M}^{pv} p_{i,h}^{pv} \Delta h + \gamma \sum_{i\in\mathcal{N}} \left(\omega_1 ({q_i}^{comp})^2 + \omega_2 {q_i}^{comp} + \omega_3\right) {q_i}^{comp}. \tag{3}$$

where:

- z_1 represents annual energy purchase costs at the substation $(USD/year)$.
- z_2 includes PV investment and O&M cost.
- C_{kWh} is the average energy cost at the substation.
- T is the total number of days in a year.
- f_a is the annualization factor that converts the initial capital costs into the equivalent annual costs.
- f_c is the anticipated cumulative energy acquisition costs throughout the project period.
- $p_{i,h}^{cg}$ is PV generation (kW) at the slack bus connected to node i at a specific time h.
- Δh is the time interval used to represent operational data for a single day.
- C_{pv} is the installed cost per capacity unit of the photovoltaic systems (USD/kWp).
- p_i^{pv} is the total installed capacity of the PV systems.
- $C_{O\&M}^{pv}$ is the O&M cost of the PV sources.
- γ represents the capital annualization factor for reactive power compensation investments.
- $\mathcal{H}, \mathcal{N}$ and T denote the sets of daily periods, network nodes, and analyzed years, respectively.
- ω_1, ω_2 and ω_3 denote the cubic, quadratic, and linear cost coefficients for the installation of a D-STATCOM with nominal capacity q_i^{comp} at bus i.

2.2. Constraints

The constraints guarantee system feasibility and reliable operation. They are classified as follows:

2.2.1. Power flow equations:

$$p_{i,h}^{cg} + p_{i,h}^{pv} - P_{i,h}^{d} = v_{i,h} \sum_{j \in \mathcal{N}} Y_{ij} v_{j,h} \cos(\theta_{i,h} - \theta_{j,h} - \varphi_{ij}), \tag{4}$$

$$q_{i,h}^{cg} + q_{i,h}^{comp} - Q_{i,h}^{d} = v_{i,h} \sum_{j \in \mathcal{N}} Y_{ij} v_{j,h} \sin(\theta_{i,h} - \theta_{j,h} - \varphi_{ij}). \tag{5}$$

2.2.2. Power generation bounds:

$$P_i^{cg,\min} \leq p_{i,h}^{cg} \leq P_i^{cg,\max}, \tag{6}$$

$$Q_i^{cg,\min} \leq q_{i,h}^{cg} \leq Q_i^{cg,\max}, \tag{7}$$

$$x_i^{pv} P_{i,h}^{pv,\min} \leq p_i^{pv} \leq x_i^{pv} P_{i,h}^{pv,\max}, \tag{8}$$

$$p_{i,h}^{pv} = G_{i,h}^{pv} p_i^{pv}. \tag{9}$$

2.2.3. Voltage regulation:

$$v^{\min} \leq v_{i,h} \leq v^{\max}. \tag{10}$$

2.2.4. Device installation constraints:

$$\sum_{i \in \mathcal{N}} x_i^{pv} \leq N_{pv}^{ava}, \tag{11}$$

$$x_i^{comp} Q_i^{comp,\min} \leq q_i^{comp} \leq x_i^{comp} Q_{i,h}^{comp,\max}, \tag{12}$$

$$q_{i,h}^{comp} = q_i^{comp}, \tag{13}$$

$$\sum_{i \in \mathcal{N}} x_i^{comp} \leq N_{comp}^{ava}. \tag{14}$$

2.2.5. Annualization and energy costs: The annualization factor f_a converts capital costs to annual equivalents, while f_c represents the projected cumulative costs of energy purchasing over the project duration. These link capital operational costs to the objective function z_1 and z_2.

$$f_a = \frac{t_a}{1-(1+t_a)^{-N_t}}, \tag{15}$$

$$f_c = \sum_{t\in\mathcal{T}} \left(\frac{1+t_e}{1+t_a}\right)^t. \tag{16}$$

where

- t_a represents the fixed investment return rate assumed for the network owner or operator throughout the planning period.
- N_t denotes the project lifetime, measured in years.
- t_e denotes the expected annual escalation rate of energy procurement costs over the 20-year planning period.
- $\mathcal{T}$ contains all years in the planning period.

2.3. Model characteristics

The mathematical model integrates non-convex, convex, and binary components, which reflects the complexity of the optimization problem. A detailed description of the model's characteristics is presented below:

- **Non-convex components:** The Objective Function (1) and the Equality Constraints (4) and (5) manifest nonlinear and non-convex properties. At first, this components arise because of the inclusion of trigonometric functions -sine and cosine functions- the interactions among voltage variables and the cubic expressions.
- **Convex components:** A group of equations from the model are characterized by a lineal and convex behavior, including the Inequality Constraints (6), (7), and (10), in addition to the Equality Constraints (9) and (13). These constraints primarily manifest the upper and lower bounds of the decision variables.
- **Binary components:** The binary characteristic of the model is shown by the Inequalities (8), (11), (12), and (14). These constraints indicate if specific actions like the installation of PVs or D-STATCOMs could be implemented in the system. These constraints involve discrete decision variables.

As can be observed, Equations (15) and (16) aren't included in this classification because they provide constant parameters associated with annualization and projected energy costs for the project´s duration.

3. Solution strategy

The optimization problem described by equations (1)–(14) is inherently complex due to its nonlinear, mixed-integer nature. To effectively address this challenge, a two-stage solution strategy is employed, comprising a master stage and a slave stage. In the master stage, the Fractional Optimization Algorithm (FOA) is utilized to identify optimal locations and sizes for PVs and D-STATCOMs. Subsequently, the slave stage verifies the feasibility and accuracy of these solutions through detailed power flow analysis. This iterative process ensures that the proposed configurations are both economically optimal and operationally reliable. The following sections elaborate on the main components of this methodology, with particular emphasis on the power flow solution in the slave stage.

3.1. Slave stage: power flow solution

The successive approximations method is used to evaluate the results obtained from the master stage (*i.e.*, the FOA). This method is formulated with a complex variable representation and has the property to solve nonlinear equality constraints associated with power balance. Solving iteratively the system of equations described by (4)

and (5), and assuming a fixed power injection and demand, the power flow method computes all voltage profiles-in fact this is its primary purpose.

Equation (17) defines the iterative structure, which serves as the core of the successive approximations method [7]. This equation reformulates the nonlinear power balance Equations (4) and (5) in matrix form as follows: :

$$\mathbb{V}_{d,h}^{t+1} = -\mathbb{Y}_{d,d}^{-1}\left[\text{diag}^{-1}\left(\mathbb{V}_{d,h}^{t,\star}\right)\mathbb{S}_{d,h}^{\star} - \mathbb{Y}_{d,g}\mathbb{V}_{g,h}\right], \tag{17}$$

where:

- $\mathbb{V}_{d,h}^{t+1}$ is the vector containing the voltages at all the demand nodes for the period h during iteration $t+1$.
- $\mathbb{Y}_{d,d}^{-1}$ is the inverse of the sub-matrix of the nodal admittance matrix corresponding to the demand nodes.
- $\mathbb{S}_{d,h}^{\star}$ represents the net complex power at demand nodes, incorporating power injections from DERs and loads:
$$\mathbb{S}_{d,h}^{\star} = \mathbb{S}_{d,h}^{dg} + \mathbb{S}_{DERs,h}^{b} - \mathbb{S}_{d,h}^{d}.$$
- Here, $\mathbb{S}_{d,h}^{dg}$ refers to conventional DG, $\mathbb{S}_{DERs,h}^{b}$ denotes the power injected by the PVs and D-STATCOMs, and $\mathbb{S}_{d,h}^{d}$ represents the demand.
- $\mathbb{Y}_{d,g}$ is the rectangular sub-matrix of the admittance matrix linking the slack bus to the demand nodes.
- $\mathbb{V}_{g,h}$ is the voltage at the slack bus, which is assumed to be fixed and equal to the nominal substation voltage.

The nodal admittance matrix Y_{bus} is constructed from Table 1 branch data: $Y_{ii} = \sum(1/Z_{ij})$, $Y_{ij} = -1/Z_{ij}$ for each branch (i,j) with $Z_{ij} = R_{ij} + jX_{ij}$. Sub-matrices: $Y_{d,d}$ (demand nodes 2-N), $Y_{d,g}$ (demand-to-slack).

There is a criterion given in Equation (18), which represents the stopping when the convergence of the successive approximations method is satisfied. A predefined tolerance ε (set at 1×10^{-10}) is compared with the maximum voltage deviation between iterations [21]:

$$\max_{h}\left|\mathbb{V}_{d,h}^{t+1} - \mathbb{V}_{d,h}^{t}\right| \leq \varepsilon, \quad \forall h \in \mathcal{H}. \tag{18}$$

Equation (19) is used to determine the power injected by the slack bus at every time period h, when the iterative process appears to have converged. It occurs when the stopping criterion represented in Equation (18) is satisfied [4]:

$$\mathbb{S}_{g,h} = \mathbb{Y}_{d,g}\mathbb{V}_{g,h} + \mathbb{Y}_{g,d}\mathbb{V}_{d,h}, \quad \forall h \in \mathcal{H}, \tag{19}$$

where $\mathbb{S}_{g,h}$ represents the complex power vector injected by the slack bus at each time period h. This final step validates feasibility and consistency of the solution with system constraints ensuring that all electrical parameters -power flows and voltage profiles- are aligned with the proposed solution.

3.2. Master stage: the FOA approach

The *fractional optimization algorithm* (*i.e.*, the FOA) is a novel metaheuristic technique that takes its inspiration from fractional mathematical functions. To use the distinctive characteristics of these functions, FOA enhances the search process by efficiently balancing global exploration with local exploitation. As a math-inspired optimization method, FOA is highly suitable for solving complex continuous optimization problems that require navigating intricate solution spaces.

Figure 1 shows the behavior of functions in the cartesian plane, considering that both functions are fractional. The first function is (f1(x)=$\frac{2}{x^2+2}$) which has a decay towards zero. This behavior enables the solution space to have a focused exploitation. On the other hand, the second function (f2(x)=$\frac{4x}{x^2+4}$) offers a smooth variation around the origin of coordinates with values ranging between 1 and -1 along y-axis. As observed, these functions present complementary behaviors, and it is used by FOA. The FOA efficiently identifies optimal or near-optimal solutions.

The fundamental procedure of FOA consists of iterative application of fractional transformations to candidate solutions that guide their movements or trajectories depending on the objective function and constraints. This procedure enables FOA to adapt flexibly in various optimizations environments which promotes robust application performance.

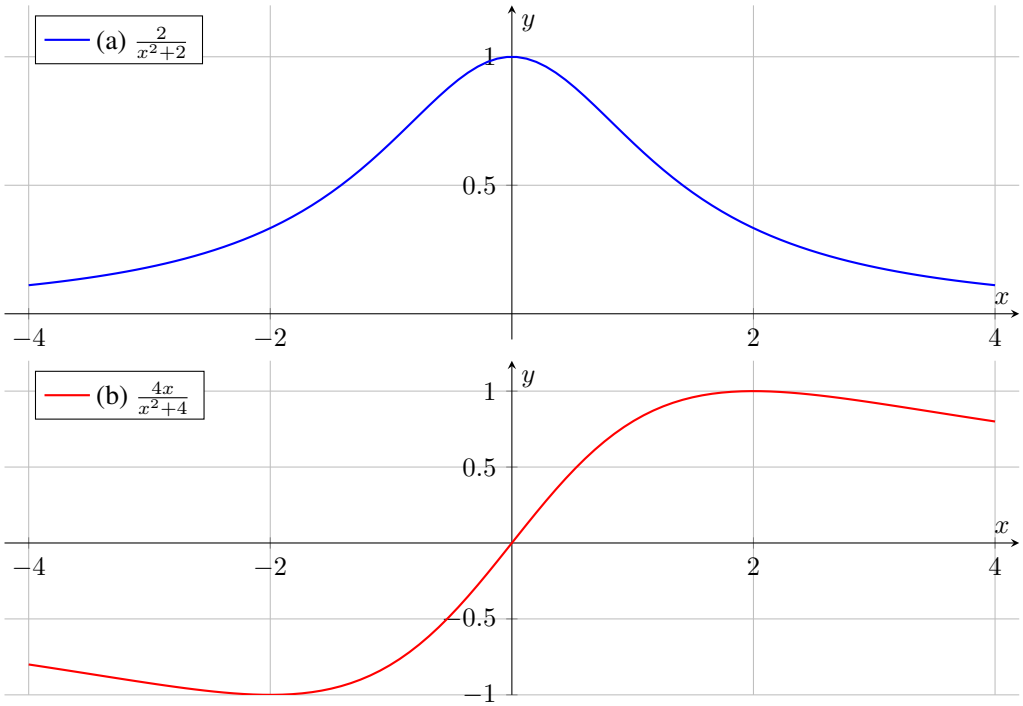

Figure 1. Graphical representation of the $\frac{2}{x^2+2}$ and $\frac{4x}{x^2+4}$ functions: (a) $\frac{2}{x^2+2}$, and (b) $\frac{4x}{x^2+4}$

3.2.1. Problem encoding and initial population As previously discussed, the decision variables of the optimization problem are associated with the optimal placement and sizing of PVs and D-STATCOMs units in a distribution network with 33 and 69 buses. To illustrate it, a specific example is proposed. Consider a network with 33 buses, where the formulation involves two PVs and two D-STATCOMs with maximum capacities of 1000 kW and 700 kvar, respectively. The candidate solution vector is presented as follows:

$$x_j = \begin{bmatrix} 25 & 28 & 3 & 31 & 736.98 & 918.30 & 505.69 & 618.51 \end{bmatrix}, \tag{20}$$

The candidate solution vector interpretation is presented:

i. The two PV units are located at buses 25 and 28, with nominal capacities of 736.98 kW and 918.30 kW, respectively.
ii. The two D-STATCOMs units are located at buses 3 and 31, with nominal capacities of 505.69 kvar and 618.51 kvar, respectively.

This hybrid master-slave optimization strategy employs a maximum of three PVs and three D-STATCOMs, so the candidate solution vector consists of three optimal placements and sizing variables for PVs and three optimal placement and sizing variables for D-STATCOMs. In the experiments, the PV units were limited to a maximum capacity of 2400 kW, while the D-STATCOMs were limited to 2000 kvar.

The candidate solution vector x_j corresponds to the j^{th} candidate solution at iteration p inside the population. The population is represented by a matrix designated as X^p with dimensions $n_s \times n_v$, where n_v represents the variables related to placement and sizing of the PVs and D-STATCOMs units in the network, and n_s is the total number of candidate solutions. This encoding strategy allows each candidate solution to have a unique siting and sizing configuration, thereby facilitating the effective exploration and exploitation of the solution space throughout the optimization process.

Following the rule defined in Equation (21), the values of the decision variables are generated. This procedure initializes every candidate solution x_j^p for the first iteration, where ($p = 0$):

$$x_{j,l} = x_l^{\min} + \beta_l \left(x_l^{\max} - x_l^{\min} \right), \quad \begin{Bmatrix} l = 1, 2, \ldots, n_v \\ j = 1, 2, \ldots, n_s \end{Bmatrix}, \tag{21}$$

where:

- β_l is an aleatory variable extracted from a uniform distribution over the interval $[0, 1]$, making sure that a diverse and stochastic initialization of decision variables is made.
- $x_l^{\min}$ and $x_l^{\max}$ define the viable search space, where $x_l^{\min}$ represents the lower bound and $x_l^{\max}$ the upper bound of the l^{th} decision variable.

This encoding approach has the potential to promote an effective exploration and exploitation of the solution space throughout the optimization process, as it guarantees that each decision variable in the candidate solution remains within its predefined limits. The initialization provided by the variable β_l allows the algorithm to begin with a set of solutions, that is essential for global optimization.

3.2.2. Exploration and exploitation rules The next step after initializing the population X^p is to identify x_{best}^p, which denotes the best solution within it.

At an iteration p, all the candidate solutions n_s in the population X^p are evaluated in the objective function to determine the optimal solution. By the equation (22), this process determines the value that minimizes the best solution:

$$x_{\text{best}}^p = \left\{ x_j^p \mid x_j^p = \arg\min \left(F_f \left(x_j^p \right) \right), \ \forall j = 1, 2, \ldots, n_s \right\}, \tag{22}$$

where $F_f \left(x_j^p \right)$ represents the fitness function value, which is associated with x_j^p, and x_j^p is the j^{th} solution at iteration p.

Constraints are enforced via feasible solution rejection in the slave stage. The successive approximations power flow (equations (17)-(19)) validates operational feasibility $V \in [0.95, 1.05]$ pu. Infeasible configurations produce invalid slack injections $Sgen$, naturally yielding high fitness values and rejection by the FOA master stage. Equation (23) shows the fitness function that is simplified to:

$$F_f(x) = z_{\text{cost}}, \tag{23}$$

where only feasible solutions contribute to optimization.

At the current iteration, the update rule described in Equation (24) is applied to all candidate solutions $\forall k = 1, 2, \ldots, n_s$, once the best solution has been identified:

$$y_j^p = \begin{cases} x_j^p + \alpha_1 \cdot \frac{2}{\alpha_2^2+2} \cdot \left(\alpha_3 x_{\text{best}}^p - (1-\alpha_3) x_j^p \right), & \beta \leq \frac{1}{2}, \\ x_j^p + \alpha_1 \cdot \frac{4\alpha_2}{\alpha_2^2+4} \cdot \left| \alpha_3 x_{\text{best}}^p - (1-\alpha_3) x_j^p \right|, & \beta > \frac{1}{2}. \end{cases} \tag{24}$$

In Equation (24) the notation $\alpha_1 \cdot \frac{2}{\alpha_2^2+2}$ means that there is an element-wise product between the vectors α_1 and $\frac{2}{\alpha_2^2+2}$. The term y_j^p denotes the update candidate solution for the next iteration. α_1 is a linear decay function. α_2 is a vector with dimensions $1 \times n_v$, which is composed of uniformly distributed values within the range $[-4, 4]$; these values are random. α_3 and β are random values uniformly distributed within $[0, 1]$. α_3 determines the level of influence that has the best candidate in the population on the current solution.

Finally, it is important to note that the absolute value is not applied for $\frac{2}{\alpha_2^2+2}$, since the values of this function vary between the range $[0, 1]$. However, the function $\frac{4\alpha_2}{\alpha_2^2+4}$ requires the absolute value consideration because of it is bounded within ± 1.

α_1, which is a linear decay function, is updated at each iteration as expressed by the following equation:

$$\alpha_1 = a\left(1 - \frac{p}{p_{\max}}\right), \tag{25}$$

where a is a scaling factor that is defined by the user and the recommendation for this value is commonly referred to 2, *i.e.*, $a = 2$ [22]. $p_{\max}$ denotes the total number of iterations.

The candidate solution y_k^p has to be evaluated because of it must adhere to the bounds of the decision variables that were predefined. The variable will be corrected if violates these bounds as specified in Equation (26) shows. It is applied for all $j = 1, 2, \ldots, n_v$ and $l = 1, 2, \ldots, n_s$:

$$y_{j,l}^p = \begin{cases} y_{j,l}, & \text{if } x_l^{\min} \leq y_{j,l} \leq x_l^{\max}, \\ x_l^{\min}, & \text{if } y_{j,l} < x_l^{\min}, \\ x_l^{\max}, & \text{if } y_{j,l} > x_l^{\max}. \end{cases} \tag{26}$$

This correction is implemented to maintain the feasibility of the solution, which allows that any variable that exceeds the bounds is set to the nearest permissible value.

3.2.3. Population substitution Once the new candidate solutions (y_k^p) have been generated, the encoding strategy determines if they will be included in the population for the next iteration. Based on the performance function value $F_f\left(y_j^p\right)$, the replacement rule is defined in the equation (27) and shown below:

$$x_j^{p+1} = \begin{cases} y_j^p, & F_f\left(y_j^p\right) < F_f\left(x_j^p\right) \\ x_j^p, & F_f\left(y_j^p\right) \geq F_f\left(x_j^p\right) \end{cases}, \quad \forall j = 1, 2, ..., n_s. \tag{27}$$

This rule replaces existing solutions with new candidate solutions if their performance is better than that of the existing ones, according to the fitness function.

3.2.4. Stopping criteria There are two common stopping criteria that are frequently employed in the literature for metaheuristic optimization techniques. The first is when the optimization algorithm finishes after the number of the iterations defined by the user is reached. The second occurs when there is no improvement in the objective function for $k_{\max}$ consecutive iterations. When the optimization technique uses the second criterion, there is a counter that is implemented to track the number of iterations without improvement in the objective function. The user defines the parameter $k_{\max}$, which represents the maximum number of non-improving iterations.

4. Test feeders and model characterization

IEEE standard feeders validate against literature. Limitations: only radial topology. The single-line diagrams of the 33- and 69-bus test feeders [7] are shown in Figure 2, and their electrical characteristics are described in Table 1. These systems were used to determine the optimal placement and sizing of PVs and D-STATCOMs using the FOA. They are designed to operate at a nominal voltage of 12,660 V at the substation level and have a radial configuration.

In this way, this method was evaluated using the daily power consumption (active and power demand curves), along with solar generation behavior [20]. Figure 3 shows the 24-hour daily profiles used in the MINLP model: active power demand, reactive power demand and solar generation. Peak demand occurs at approximately $20h$, while solar peaks at midday (approximately $12h$). These deterministic profiles validate the multi-period optimization over $h \in [1, 24]$, enabling realistic annual cost computation z_1. Future work will incorporate uncertainty scenarios per reviewer suggestions.

The parameters associated with the PV units are presented in Table 2. On the other hand, Table 3 details the costs related to the D-STATCOM units.

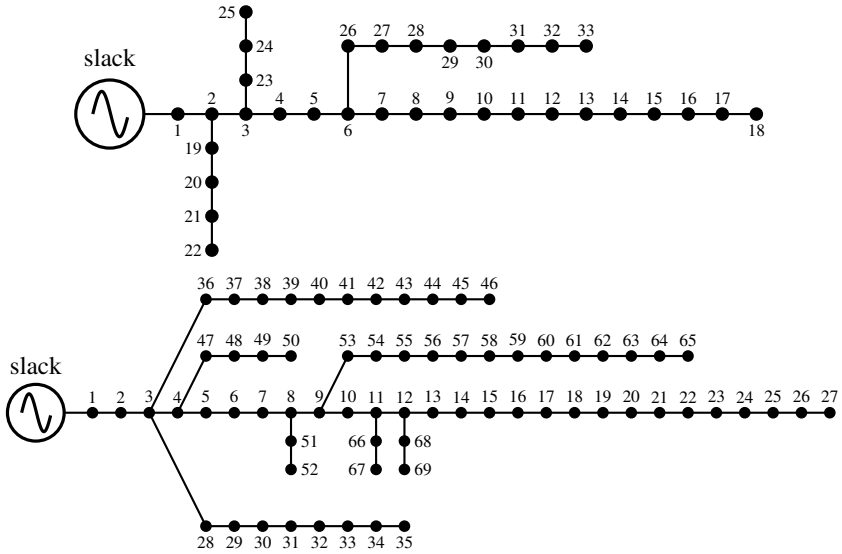

Figure 2. Single-line diagrams of the 33- and 69-bus test feeders

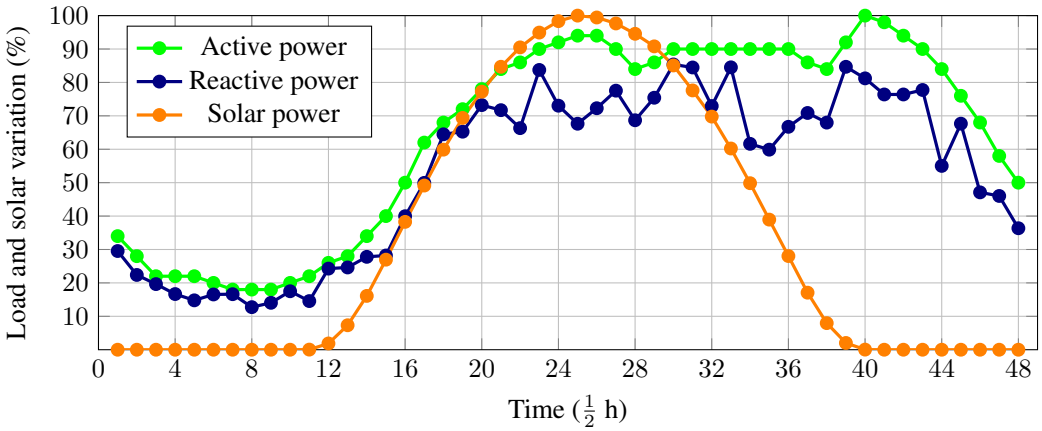

Figure 3. Daily power consumption and solar generation behavior

5. Numerical assessment

The FOA was implemented in MATLAB R2024a and executed over 100 independent runs, a population size $ns = 50$ and maximum iterations $p_{max} = 1000$ per run, to ensure statistical robustness. The programming code was specifically developed to implement the SCA method and the successive approximations power flow method, while the VSA was performed and compared. VSA was used as described in [20]. Reported metrics use best-of-100 solutions from Tables 4-5. All simulations used Intel i3-1115G4, 8GB RAM

5.1. Results for the 33-bus grid

Table 4 presents comparative analysis of the proposed solution method for the 33-bus grid.

Based on the values given in Table 4, the FOA achieved the best overall performance for the 33-bus feeder, yielding the lowest total project cost among the compared algorithms.

Table 1. Branch and load data for the 33- and 69-bus grids

The 33-bus grid											
Node i	**Node j**	**R_{ij} (Ω)**	**X_{ij} (Ω)**	**P_j (kW)**	**Q_j (kvar)**	**Node i**	**Node j**	**R_{ij} (Ω)**	**X_{ij} (Ω)**	**P_j (kW)**	**Q_j (kvar)**
1	2	0.0922	0.0477	100	60	17	18	0.7320	0.5740	90	40
2	3	0.4930	0.2511	90	40	2	19	0.1640	0.1565	90	40
3	4	0.3660	0.1864	120	80	19	20	1.5042	1.3554	90	40
4	5	0.3811	0.1941	60	30	20	21	0.4095	0.4784	90	40
5	6	0.8190	0.7070	60	20	21	22	0.7089	0.9373	90	40
6	7	0.1872	0.6188	200	100	3	23	0.4512	0.3083	90	50
7	8	1.7114	1.2351	200	100	23	24	0.8980	0.7091	420	200
8	9	1.0300	0.7400	60	20	24	25	0.8960	0.7011	420	200
9	10	1.0400	0.7400	60	20	6	26	0.2030	0.1034	60	25
10	11	0.1966	0.0650	45	30	26	27	0.2842	0.1447	60	25
11	12	0.3744	0.1238	60	35	27	28	1.0590	0.9337	60	20
12	13	1.4680	1.1550	60	35	28	29	0.8042	0.7006	120	70
13	14	0.5416	0.7129	120	80	29	30	0.5075	0.2585	200	600
14	15	0.5910	0.5260	60	10	30	31	0.9744	0.9630	150	70
15	16	0.7463	0.5450	60	20	31	32	0.3105	0.3619	210	100
16	17	1.2860	1.7210	60	20	32	33	0.3410	0.5302	60	40
The 69-bus grid											
Node i	**Node j**	**R_{ij} (Ω)**	**X_{ij} (Ω)**	**P_j (kW)**	**Q_j (kvar)**	**Node i**	**Node j**	**R_{ij} (Ω)**	**X_{ij} (Ω)**	**P_j (kW)**	**Q_j (kvar)**
1	2	0.0005	0.0012	0.00	0.00	3	36	0.0044	0.0108	26.00	18.55
2	3	0.0005	0.0012	0.00	0.00	36	37	0.0640	0.1565	26.00	18.55
3	4	0.0015	0.0036	0.00	0.00	37	38	0.1053	0.1230	0.00	0.00
4	5	0.0251	0.0294	0.00	0.00	38	39	0.0304	0.0355	24.00	17.00
5	6	0.3660	0.1864	2.60	2.20	39	40	0.0018	0.0021	24.00	17.00
6	7	0.3810	0.1941	40.40	30.00	40	41	0.7283	0.8509	1.20	1.00
7	8	0.0922	0.0470	75.00	54.00	41	42	0.3100	0.3623	0.00	0.00
8	9	0.0493	0.0251	30.00	22.00	42	43	0.0410	0.0478	6.00	4.30
9	10	0.8190	0.2707	28.00	19.00	43	44	0.0092	0.0116	0.00	0.00
10	11	0.1872	0.0619	145.00	104.00	44	45	0.1089	0.1373	39.22	26.30
11	12	0.7114	0.2351	145.00	104.00	45	46	0.0009	0.0012	29.22	26.30
12	13	1.0300	0.3400	8.00	5.00	4	47	0.0034	0.0084	0.00	0.00
13	14	1.0440	0.3450	8.00	5.50	47	48	0.0851	0.2083	79.00	56.40
14	15	1.0580	0.3496	0.00	0.00	48	49	0.2898	0.7091	384.70	274.50
15	16	0.1966	0.0650	45.50	30.00	49	50	0.0822	0.2011	384.70	274.50
16	17	0.3744	0.1238	60.00	35.00	8	51	0.0928	0.0473	40.50	28.30
17	18	0.0047	0.0016	60.00	35.00	51	52	0.3319	0.1114	3.60	2.70
18	19	0.3276	0.1083	0.00	0.00	9	53	0.1740	0.0886	4.35	3.50
19	20	0.2106	0.0690	1.00	0.60	53	54	0.2030	0.1034	26.40	19.00
20	21	0.3416	0.1129	114.00	81.00	54	55	0.2842	0.1447	24.00	17.20
21	22	0.0140	0.0046	5.00	3.50	55	56	0.2813	0.1433	0.00	0.00
22	23	0.1591	0.0526	0.00	0.00	56	57	1.5900	0.5337	0.00	0.00
23	24	0.3463	0.1145	28.00	20.00	57	58	0.7837	0.2630	0.00	0.00
24	25	0.7488	0.2475	0.00	0.00	58	59	0.3042	0.1006	100.00	72.00
25	26	0.3089	0.1021	14.00	10.00	59	60	0.3861	0.1172	0.00	0.00
26	27	0.1732	0.0572	14.00	10.00	60	61	0.5075	0.2585	1244.00	888.00
3	28	0.0044	0.0108	26.00	18.60	61	62	0.0974	0.0496	32.00	23.00
28	29	0.0640	0.1565	26.00	18.60	62	63	0.1450	0.0738	0.00	0.00
29	30	0.3978	0.1315	0.00	0.00	63	64	0.7105	0.3619	227.00	162.00
30	31	0.0702	0.0232	0.00	0.00	64	65	1.0410	0.5302	59.00	42.00
31	32	0.3510	0.1160	0.00	0.00	11	66	0.2012	0.0611	18.00	13.00
32	33	0.8390	0.2816	14.00	10.00	66	67	0.0470	0.0140	18.00	13.00
33	34	1.7080	0.5646	19.50	14.00	12	68	0.7394	0.2444	28.00	20.00
34	35	1.4740	0.4873	6.00	4.00	68	69	0.0047	0.0016	28.00	20.00

Table 2. Parameters associated with the optimal location and capacity of PVs in distribution networks

Parameter	**Value**	**Unit**	**Parameter**	**Value**	**Unit**
C_{kWh}	0.1390	USD/kWh	T	365	days
t_a	10	%	N_t	20	years
Δh	1	h	t_e	2	%
C_{pv}	1036.49	USD/kWp	C_{0andM}	0.0019	USD/kWh
N_{pv}^{ava}	3	-	$p_i^{pv,\max}$	2400	kW
$P_k^{pv,\min}$	0	kW			

Table 3. Parameters associated with the cost data for the D-STATCOM devices

Parameter	Value	Unit	Parameter	Value	Unit
ω_1	0.30	USD/Mvar^3	ω_2	-305.10	USD/Mvar^2
ω_3	127,380	USD/Mvar	γ	1/20	—
$Q_i^{comp,\min}$	0	Mvar	$Q_{i,h}^{comp,\max}$	2000	kvar
$P_i^{cg,\min}$	0	W	$P_i^{cg,\max}$	5000	kW
$Q_i^{cg,\min}$	0	var	$Q_i^{cg,\max}$	5000	kvar

Table 4. Numerical results obtained in the 33-bus grid

Scen.	x_i^{comp} (Node)	q_i^{comp} (Mvar)	x_i^{pv} (Node)	p_i^{pv} (MW)	A_{cost_3} (USD)	Ave. time (s)
Benchmark case	—	—	—	—	3,553,557.38	—
VSA	[6, 15, 31]	[0.3801, 0.0640, 0.3543]	[9, 14, 31]	[0.9844, 0.6312, 1.7602]	2,292,022.62	305.36
SCA	[11, 12, 30]	[0.0092, 0.1143, 0.4617]	[7, 14, 31]	[0.4348, 1.8842, 1.0836]	2,291,234.65	305.97
FOA	[30, 18, 11]	[0.4447, 0.0499, 0.0993]	[12, 17, 31]	[1.4857, 0.3639, 1.5403]	2,290.366.39	203.20

i. In terms of cost optimization, the FOA reached a total value of $2,290,366.39, representing a reduction of approximately 35.55% relative to the benchmark case. This outcome outperformed the SCA ($2,291,234.65) and the VSA ($2,292,022.62), producing additional savings of $868.26 and $1,656.23, respectively. These results confirm the FOA's superior capability to reduce costs in this scenario.
ii. Regarding PV placement, the FOA determined that buses 12, 17, and 31 offered the most advantageous locations, with installed capacities of 1485.7 kW, 363.9 kW, and 1540.3 kW, respectively. These differ from the configurations obtained by the SCA and VSA but emphasize the suitability of these nodes for integrating renewable generation. For D-STATCOM placement, the FOA selected buses 30, 18, and 11, assigning reactive power capacities of 444.7 kvar, 49.9 kvar, and 99.3 kvar.
iii. The FOA also demostrates competitive computational performance, with an average execution time of 203.20 s. While slower than that of the SCA (305.97 s) and the VSA (305.36 s), this significant reduction highlights an important advantage, as it shows that considerable processing time can be saved.

5.2. Results for the 69-bus grid

Table 5 presents comparative analysis of the proposed solution method for the 69-bus grid.

Table 5. Numerical results obtained in the 69-bus grid

Scen.	x_i^{comp} (Node)	q_i^{comp} (Mvar)	x_i^{pv} (Node)	p_i^{pv} (MW)	A_{cost_3} (USD)	Ave. time (s)
Benchmark case	—	—	—	—	3,723,529.52	—
VSA	[19, 53, 63]	[0.0871, 0.0075, 0.4555]	[15, 33, 62]	[0.8753, 0.5941, 2.0184]	2,400,490.65	1680.10
SCA	[7, 61, 65]	[0.0337, 0.3992, 0.1076]	[18, 59, 61]	[0.8761, 0.3407, 2.2949]	2,396,720.37	1611.16
FOA	[61, 42, 19]	[0.4951, 0.0375, 0.1225]	[22, 61, 64]	[0.4945, 1.9647, 1.0779]	2,395,198.51	2001.01

The numerical evidence confirms that the FOA offers significant advantages when applied to the 69-bus distribution network under study. The main observations are summarized as follows:

i. The FOA achieved the smallest total cost among all compared optimization methods, with a value of $2,395,198.51, corresponding to a 35.674% reduction relative to the benchmark case ($3,723,529.52). This translates into savings of $1,328,331.01 compared to the benchmark, $1,521.86 compared to the SCA ($2,396,720.37), and $5,292.14 compared to the VSA ($2,400,490.65). These results emphasize its clear advantage in minimizing costs.
ii. The FOA identified buses 22, 61, and 64 as the best locations, assigning capacities of 494.5 kW, 1,964.7 kW, and 1,078.0 kW, respectively. Unlike the SCA and VSA, which chose different nodes and showed wider variations in sizing, the FOA's selection achieves a more evenly distributed generation layout — a feature that can support improved grid stability and operational efficiency.
iii. The FOA positioned the D-STATCOM units at buses 61, 42, and 19, with reactive power capacities of 495.51 kvar, 37.5 kvar, and 122.58 kvar, respectively. Moreover, the FOA's overall allocation differs from

that obtained by the SCA and VSA, while also delivering a higher total reactive power capacity — further reinforcing its effectiveness in improving operational reliability. Notably, bus 61 appears as a common optimal location for both PV installation and D-STATCOM placement, underscoring its strategic role in enhancing the network's performance.

iv. In terms of computational performance, the FOA required an average runtime of 2001.01 s. Although this value is higher in comparison with the SCA (1611.16 s) and the VSA (1680.10 s), the additional computational effort is justified by the superior results achieved by the FOA.

In short, the FOA not only reduces project costs but also delivers a balanced and effective allocation of PV and D-STATCOM resources. These results validate it as a robust and dependable optimization approach for complex distribution network problems, particularly in scenarios that demand both efficiency and feasibility.

6. Conclusions and future work

The FOA proved to be a highly effective tool for reducing project costs in both the 33- and 69-bus distribution networks. Across all tests, it consistently outperformed the SCA and the VSA, showing a clear advantage in its optimization capability. In the 33-bus case, the FOA delivered additional savings of $868.26 compared to the SCA and $1,656.23 compared to the VSA. In the 69-bus case, the margin was even greater, surpassing the SCA by $1,521.86 and the VSA by $5,292.14. These results reinforce the FOA's ability to find cost-effective solutions in challenging optimization scenarios.

Beyond cost reduction, the FOA showed strong performance in placing and sizing PV units and D-STATCOMs in ways that support both technical and economic goals. One particularly interesting outcome was in the 69-bus network, where bus 61 emerged as a common choice for both PV and D-STATCOM installation. This repeated selection highlights the strategic role of this node in providing both active and reactive power support, which in turn helps improve voltage profiles and reduce system losses.

Although the 69-bus grid requires longer processing times, the 33-bus grid shows the opposite behavior. It means that results obtained by the FOA are better in general, achieving cost reductions and robust solutions. This suggests that this algorithm is reliable and adaptable tool for optimization in DSs. In future works, its potential makes it a strong candidate for application in larger and more complex grids.

Looking ahead, there is room to explore the FOA's full potential. A broader comparison with other well-known optimization algorithms—such as particle swarm optimization, genetic algorithms, and differential evolution—would offer a more complete picture of its strengths and limitations. Hybrid strategies that combine FOA with other techniques could be another promising path, potentially improving solution quality and reducing computation time. Finally, extending the method to tackle multi-objective problems and to account for uncertainties in renewable generation and demand would bring it closer to real-world applications, where flexibility and robustness are key.

REFERENCES

1. R.A. UFA, Y.Y. Malkova, V.E. Rudnik, M.V. Andreev, and V.A. Borisov. A review on distributed generation impacts on electric power system. *International Journal of Hydrogen Energy*, 47:20347–20361, June 2022.
2. Mahmoud Pesaran H.A, Phung Dang Huy, and Vigna K. Ramachandaramurthy. A review of the optimal allocation of distributed generation: Objectives, constraints, methods, and algorithms. *Renewable and Sustainable Energy Reviews*, 75:293–312, August 2017.
3. Kola Sampangi Sambaiah. A review on optimal allocation and sizing techniques for dg in distribution systems. *INTERNATIONAL JOURNAL of RENEWABLE ENERGY RESEARCHS*, 8(3), September 2018.
4. Oscar Danilo Montoya, Luis Fernando Grisales-Noreña, and Walter Gil-González. Simultaneous siting and sizing of pvs and d-statcoms in medium-voltage grids using the cauchy-based distribution optimizer. *Results in Engineering*, 25:104407, March 2025.
5. Femke J. M. M. Nijsse, Jean-Francois Mercure, Nadia Ameli, Francesca Larosa, Sumit Kothari, Jamie Rickman, Pim Vercoulen, and Hector Pollitt. The momentum of the solar energy transition. *Nature Communications*, 14, October 2023.
6. Luis Fernando Grisales-Noreña, Daniel Sanin-Villa, and Oscar Danilo Montoya. Optimal integration of pv generators and d-statcoms into the electrical distribution system to reduce the annual investment and operational cost: A multiverse optimization algorithm and matrix power flow approach. *e-Prime - Advances in Electrical Engineering, Electronics and Energy*, 9:100747, September 2024.

7. Oscar Danilo Montoya, Walter Gil-González, and Luis Fernando Grisales-Noreña. Optimal planning of photovoltaic and distribution static compensators in medium-voltage networks via the gndo approach. *Results in Engineering*, 23:102764, September 2024.
8. Adriana Rincón-Miranda, Giselle Viviana Gantiva-Mora, and Oscar Danilo Montoya. Simultaneous integration of d-statcoms and pv sources in distribution networks to reduce annual investment and operating costs. *Computation*, 11(7), July 2023.
9. S. Devi and M. Geethanjali. Optimal location and sizing determination of distributed generation and dstatcom using particle swarm optimization algorithm. *International Journal of Electrical Power & Energy Systems*, 62:562–570, November 2014.
10. Pavlos S. Georgilakis and Nikos D. Hatziargyriou. Optimal distributed generation placement in power distribution networks: Models, methods, and future research. *IEEE Transactions on Power Systems*, 28:3420–3428, January 2013.
11. Navid Razmjooy, Mohsen Ashourian, and Zahra Foroozandeh. *Metaheuristics and Optimization in Computer and Electrical Engineering*. Springer, 2021.
12. Vivek Saxena, Saibal Manna, Saurabh Kumar Rajput, Praveen Kumar, Bhupender Sharma, Mohammed H. Alsharif, and Mun-Kyeom Kim. Navigating the complexities of distributed generation: Integration, challenges, and solutions. *Energy Reports*, 12:3302–3322, December 2024.
13. Bindeshwar Singh and Janmejay Sharma. A review on distributed generation planning. *Renewable and Sustainable Energy Reviews*, 76:529–544, September 2017.
14. Prisma Megantoro, Syahirah Abd Halim, Nor Azwan Mohamed Kamari, Lilik Jamilatul Awalin, Mohd Syukri Ali, and Hazwani Mohd Rosli. Optimizing reactive power dispatch with metaheuristic algorithms: A review of renewable distributed generation integration with intermittency considerations. *Energy Reports*, 13:397–423, June 2025.
15. Samson Ademola Adegoke, Yanxia Sun, Adesola Sunday Adegoke, and Damilola Ojeniyl. Optimal placement of distributed generation to minimize power loss and improve voltage stability. *Heliyon*, 10:e39298, November 2024.
16. Abdullah M. Shaheen, Abdullah Alassaf, Ibrahim Alsaleh, and A.M. Elsayed. Enhanced kepler optimization for efficient penetration of pv sources integrated with statcom devices in power distribution systems. *Expert Systems with Applications*, 253:124333, November 2024.
17. Sandeep Gogula and V. S. Vakula. Multi-objective harris hawks optimization algorithm for selecting best location and size of distributed generation in radial distribution system. *International Journal of Cognitive Computing in Engineering*, 5:436–452, 2024.
18. Mohammed Goda Eisa, Mohammed A. Farahat, Wael Abdelfattah, and Mohammed Elsayed Lotfy. Multi-objective optimal integration of distributed generators into distribution networks incorporated with plug-in electric vehicles using walrus optimization algorithm. *sustainability*, 16(22):9948, November 2024.
19. Luis Fernando Grisales-Noreña, Daniel Sanin-Villa, and Oscar Danilo Montoya. Optimal integration of PV generators and D-STATCOMs into the electrical distribution system to reduce the annual investment and operational cost: A multiverse optimization algorithm and matrix power flow approach. *e-Prime - Advances in Electrical Engineering, Electronics and Energy*, 9:100747, September 2024.
20. Oscar Danilo Montoya, Carlos Alberto Ramírez-Vanegas, and Luis Fernando Grisales-Noreña. A sine-cosine algorithm approach for optimal pv and d-statcom integration in distribution systems. *Statistics, Optimization & Information Computing*, 13(3):1266–1279, November 2024.
21. Oscar Danilo Montoya, Walter Gil-González, Rubén Iván Bolaños, Diego Fernando Muñoz-Torres, Jesús C. Hernández, and Luis Fernando Grisales-Noreña. Effective power coordination of besus in distribution grids via the sine-cosine algorithm. In *2024 IEEE Green Technologies Conference (GreenTech)*. IEEE, April 2024.
22. Seyedali Mirjalili. SCA: A Sine Cosine Algorithm for solving optimization problems. *Knowledge-Based Systems*, 96:120–133, March 2016.